11th World Congress on Computational Mechanics (WCCM XI)
5th European Conference on Computational Mechanics (ECCM V)
6th European Conference on Computational Fluid Dynamics (ECFD VI)
E. Oñate, J. Oliver and A. Huerta (Eds)

FREE FIELD ANALYSIS BY FEM AND CIP COMBINED METHOD

NAGAYUKI YOSHIDA

Department of Architecture, Faculty of Engineering and Design
Hosei University
2-33 Ichigaya-Tamachi, Shinjuku-Ku, Tokyo 162-0843, Japan
email: nyoshida@hosei.ac.jp
http://www.design.hosei.ac.jp/gs/english/faculty/architecture.html

Key Words: *Elastic Wave, Transmitting Boundary, CIP Method, FEM.*

Summary: In recent years, the nonlinear dynamic behavior of the foundation and soil has been studied actively. When dealing with a nonlinear problem, the Finite Element Method (FEM) is an effective and flexible technique. When applying this to the wave propagation problem of infinity or a semi-infinite elastic body, the transmission processing is needed on the boundary of an analytical area at the same time for both of the incident wave, which is incoming from the exterior to an inside, and the reflected wave which is outgoing from an inside to the exterior.

Although the viscous boundary is a typical tool for the transmission processing in the elastic wave field, it is an approximate method for more than one dimensional field. The Cubic Interpolated Propagation (CIP) method is an outstanding method which can separate the incident wave and the reflected wave by transforming the wave equation to a number of advection ones. By applying this technique to the transmission processing at the boundary of FEM domain, we can formulate a new method with high precision for the wave analysis named by FEM and CIP Combined Method.

A computational procedure is described for one dimensional problem and the analytical examples of one and two-dimensional problem are shown for the validity of the proposed method.

When we analyze wave propagation in the limited analytical region, we could model the ground by FEM and CIP Combined Method as if it were extended infinitely.

1 INTRODUCTION

The equations of motion on the three dimensional elasticity are described first, and converted to a set of advection equations next. While FEM is a general computational method to solve the equations of motion, CIP method has been developed particularly for the advection equations [1]. The main purpose of this paper is to explain the basic computational procedure on how to combine FEM with CIP method in order to realize the transmitting boundary of FEM domain. The analytical examples with one and two-dimensions are shown for the validity of a proposed method.

2 EQUATION OF MOTION IN ELASTIC BODY

The fundamental equations on motion in n dimensional elastic body ($n=1, 2, 3$) are expressed as follows.

$$\frac{\partial}{\partial t}\{\dot{u}\} = \frac{1}{\rho}[\Im]\{\sigma\}, \quad \{\dot{u}\} = \frac{\partial}{\partial t}\{u\}. \tag{1}$$

$$\{\sigma\} = [D]\{\varepsilon\} = [D][\Im]^T[u] \tag{2}$$

where $\{u\}$, $\{\sigma\}$ and $\{\varepsilon\}$ are vectors of displacement, strain and stress respectively, ρ is mass density, t is time, $[\Im]$ is the partial differential operator matrix, and $[D]$ is the material property matrix consisting of Young's modulus E and Poison's ratio ν .

<n=1>

Longitudinal: $[\Im] = \frac{\partial}{\partial x}$, $\{u\} = u_x$, $\{\sigma\} = \sigma_x$, $[D] = D_1$.

Lateral: $[\Im] = \frac{\partial}{\partial x}$, $\{u\} = u_y$, $\{\sigma\} = \tau_{xy}$, $[D] = G$.

<n=2>

In-plane: $[\Im] = \begin{bmatrix} \frac{\partial}{\partial y} & \frac{\partial}{\partial x} \end{bmatrix}$, $\{u\} = u_z$, $\{\sigma\} = \begin{Bmatrix} \tau_{yz} \\ \tau_{zx} \end{Bmatrix}$, $[D] = \begin{bmatrix} G & 0 \\ 0 & G \end{bmatrix}$.

Out of plane: $[\Im] = \begin{bmatrix} \frac{\partial}{\partial x} & 0 & \frac{\partial}{\partial y} \\ 0 & \frac{\partial}{\partial y} & \frac{\partial}{\partial x} \end{bmatrix}$, $\{u\} = \begin{Bmatrix} u_x \\ u_y \end{Bmatrix}$, $\{\sigma\} = \begin{Bmatrix} \sigma_x \\ \sigma_y \\ \tau_{xy} \end{Bmatrix}$, $[D] = \begin{bmatrix} D_1 & D_2 & 0 \\ D_2 & D_1 & 0 \\ 0 & 0 & G \end{bmatrix}$.

<n=3>

$$[\Im] = \begin{bmatrix} \frac{\partial}{\partial x} & 0 & 0 & \frac{\partial}{\partial y} & 0 & \frac{\partial}{\partial z} \\ 0 & \frac{\partial}{\partial y} & 0 & \frac{\partial}{\partial x} & \frac{\partial}{\partial z} & 0 \\ 0 & 0 & \frac{\partial}{\partial z} & 0 & \frac{\partial}{\partial y} & \frac{\partial}{\partial x} \end{bmatrix}, \quad \{u\} = \begin{Bmatrix} u_x \\ u_y \\ u_z \end{Bmatrix}, \quad \{\sigma\} = \begin{Bmatrix} \sigma_x \\ \sigma_y \\ \sigma_z \\ \tau_{xy} \\ \tau_{yz} \\ \tau_{zx} \end{Bmatrix}.$$

$$[D]=\begin{bmatrix} D_1 & D_2 & D_2 & 0 & 0 & 0 \\ D_2 & D_1 & D_2 & 0 & 0 & 0 \\ D_2 & D_2 & D_1 & 0 & 0 & 0 \\ 0 & 0 & 0 & G & 0 & 0 \\ 0 & 0 & 0 & 0 & G & 0 \\ 0 & 0 & 0 & 0 & 0 & G \end{bmatrix},$$

where $D_1=\lambda+2G=\dfrac{(1-\nu)E}{(1+\nu)(1-2\nu)}$, $D_2=\lambda=\dfrac{\nu E}{(1+\nu)(1-2\nu)}$, $G=\dfrac{E}{2(1+\nu)}$.

Substituting Eq.(2) into Eq.(1), the equations of motion in an elastic body is written as follows.

$$\frac{\partial^2}{\partial t^2}\{u\}=\frac{1}{\rho}[\Im][D][\Im]^T\{u\} \tag{3}$$

3 ADVECTION EQUATION IN ELASTIC BODY

Instead of Eq.(3), we can deal with an elastic wave field by using Eqs.(1) and (2) simultaneously [2].

$$\frac{\partial}{\partial t}\begin{Bmatrix}\{\dot{u}\}\\ \{\sigma\}\end{Bmatrix}=\begin{bmatrix}[0] & \frac{1}{\rho}[I] \\ [D] & [0]\end{bmatrix}\begin{bmatrix}[\Im]^T & [0] \\ [0] & [\Im]\end{bmatrix}\begin{Bmatrix}\{\dot{u}\}\\ \{\sigma\}\end{Bmatrix} \tag{4}$$

This equation is also expressed as follows.

$$\frac{\partial}{\partial t}\{F\}=[A][Q]\{F\} \tag{5}$$

where

$$[Q]=[q_x]\frac{\partial}{\partial x}+[q_y]\frac{\partial}{\partial y}+[q_z]\frac{\partial}{\partial z}. \tag{6}$$

Therefore, we rewrite Eq.(5) as

$$\frac{\partial}{\partial t}\{F\}=[A_x]\frac{\partial}{\partial x}\{F\}+[A_y]\frac{\partial}{\partial y}\{F\}+[A_z]\frac{\partial}{\partial z}\{F\} \tag{7}$$

where

$$[A_s]=[A][q_s],\quad s=x,y,z. \tag{8}$$

Since it is difficult to solve Eq.(7), the three dimensional problem is approximately decomposed into three independent one dimensional ones.

$$\frac{\partial}{\partial t}\{F\}=[A_s]\frac{\partial}{\partial s}\{F\},\qquad s=x,y,z \tag{9}$$

Here, we consider the farther decomposition through the eigen value problem.

By using the eigen matrix $[\varphi_s]$ of $[A_s]$, the vector $\{F\}$ can be expressed as

$$\{F\}=[\varphi_s]\{f_s\},\qquad s=x,y,z. \tag{10}$$

$$\{f_s\}=\{f_{s1},f_{s2},f_{s3},f_{s4},f_{s5},f_{s6},f_{s7},f_{s8},f_{s9}\}^T \tag{11}$$

From Eqs.(9) and (10), the advection equation is obtained.

$$\frac{\partial}{\partial t}\{f_s\} = [\varphi_s]^{-1}[A_s][\varphi_s]\frac{\partial}{\partial s}\{f_s\} = [\Lambda]\frac{\partial}{\partial s}\{f_s\} \tag{12}$$

where $[\Lambda]$ is the diagonal eigenvalue matrix as follows.

$$\mathrm{diagonal}([\Lambda]) = (c_p, -c_p, c_s, -c_s, c_s, -c_s, 0, 0, 0), \tag{13}$$

$$c_p = \sqrt{D_1/\rho}, \quad c_s = \sqrt{G/\rho}\,. \tag{14}$$

From Eq.(10), the following relation is obtained.

$$\{f_r\} = [T_{rs}]\{f_s\}, \quad [T_{rs}] = [\varphi_r]^{-1}[\varphi_s] \tag{15}$$

The transfer matrix $[T_{rs}]$ can be arranged to satisfy the following relation.

$$[T_{yx}] = [T_{zy}] = [T_{xz}] = [T] \tag{16}$$

The flow of decomposition analysis is summarized in the following.

0. The initial value $\{F\}$ at $t=0$ is converted to $\{f_x\} = [\varphi_x]^{-1}\{F\}$.
1. $\{f_x\}$ is advected during Δt in the *x*-direction by the equation: $\frac{\partial}{\partial t}\{f_x\} = [\Lambda]\frac{\partial}{\partial x}\{f_x\}$ and newly obtained $\{f_x\}$ is converted to $\{f_y\} = [T]\{f_x\}$.
2. $\{f_y\}$ is advected during Δt in the *y*-direction by the equation: $\frac{\partial}{\partial t}\{f_y\} = [\Lambda]\frac{\partial}{\partial y}\{f_y\}$ and newly obtained $\{f_y\}$ is converted to $\{f_z\} = [T]\{f_y\}$.
3. $\{f_z\}$ is advected during Δt in the *z*-direction by the equation: $\frac{\partial}{\partial t}\{f_z\} = [\Lambda]\frac{\partial}{\partial z}\{f_z\}$ and newly obtained $\{f_z\}$ is converted to $\{f_x\} = [T]\{f_z\}$.
4. $\{F\} = [\varphi_x]\{f_x\}$ obtained at the end of this step is memorized, and return to 1.

The matrices used in the above numerical flow in case of $n=3$ are shown as follows.

$$[T] = \begin{bmatrix} \alpha/2 & \alpha/2 & 1/(2\beta) & -1/(2\beta) & 0 & 0 & 1/2 & 0 & 0 \\ \alpha/2 & \alpha/2 & -1/(2\beta) & 1/(2\beta) & 0 & 0 & 1/2 & 0 & 0 \\ 0 & 0 & 0 & 0 & 1/2 & -1/2 & 0 & 0 & 1/2 \\ 0 & 0 & 0 & 0 & -1/2 & 1/2 & 0 & 0 & 1/2 \\ \beta/2 & -\beta/2 & 1/2 & 1/2 & 0 & 0 & 0 & 0 & 0 \\ -\beta/2 & \beta/2 & 1/2 & 1/2 & 0 & 0 & 0 & 0 & 0 \\ \alpha(1-\alpha) & \alpha(1-\alpha) & 0 & 0 & 0 & 0 & -\alpha & 1 & 0 \\ 1-\alpha^2 & 1-\alpha^2 & 0 & 0 & 0 & 0 & -\alpha & 0 & 0 \\ 0 & 0 & 0 & 0 & 1 & 1 & 0 & 0 & 0 \end{bmatrix} \tag{17}$$

where $\alpha = D_2/D_1 = \nu/(1-\nu), \quad \beta = \sqrt{D_1/G} = c_p/c_s = 2(1-\nu)/(1-2\nu)$.

$$[\varphi_x]^{-1} = \begin{bmatrix} 1/(2c_p) & 0 & 0 & 1/(2D_1) & 0 & 0 & 0 & 0 & 0 \\ -1/(2c_p) & 0 & 0 & 1/(2D_1) & 0 & 0 & 0 & 0 & 0 \\ 0 & 1/(2c_s) & 0 & 0 & 0 & 0 & 1/(2G) & 0 & 0 \\ 0 & -1/(2c_s) & 0 & 0 & 0 & 0 & 1/(2G) & 0 & 0 \\ 0 & 0 & 1/(2c_s) & 0 & 0 & 0 & 0 & 0 & 1/(2G) \\ 0 & 0 & -1/(2c_s) & 0 & 0 & 0 & 0 & 0 & 1/(2G) \\ 0 & 0 & 0 & -\alpha/D_1 & 1/D_1 & 0 & 0 & 0 & 0 \\ 0 & 0 & 0 & -\alpha/D_1 & 0 & 1/D_1 & 0 & 0 & 0 \\ 0 & 0 & 0 & 0 & 0 & 0 & 0 & 1/G & 0 \end{bmatrix}, \qquad (18)$$

$$[\varphi_x] = \begin{bmatrix} c_p & -c_p & 0 & 0 & 0 & 0 & 0 & 0 & 0 \\ 0 & 0 & c_s & -c_s & 0 & 0 & 0 & 0 & 0 \\ 0 & 0 & 0 & 0 & c_s & -c_s & 0 & 0 & 0 \\ D_1 & D_1 & 0 & 0 & 0 & 0 & 0 & 0 & 0 \\ D_2 & D_2 & 0 & 0 & 0 & 0 & D_1 & 0 & 0 \\ D_2 & D_2 & 0 & 0 & 0 & 0 & 0 & D_1 & 0 \\ 0 & 0 & G & G & 0 & 0 & 0 & 0 & 0 \\ 0 & 0 & 0 & 0 & 0 & 0 & 0 & 0 & G \\ 0 & 0 & 0 & 0 & G & G & 0 & 0 & 0 \end{bmatrix}. \qquad (19)$$

4 CIP METHOD FOR ADVECTION EQUATION

CIP method is an effective numerical tool to solve the advection equation with high accuracy. For later explanations, we here quote the formulation written by Yabe *et al*. [3] as below:

"If two values of f and g are given at two grid points, the profile between these points can be interpolated by cubic polynomial $F(x) = as^3 + bs^2 + cs + d$.

Thus, the profile at $n+1$-step can be obtained shifting the profile by $c\Delta t$ such as $f^{n+1} = F(s - c\Delta t)$, $g^{n+1} = dF(s - c\Delta t)/ds$.

$$a_i = \frac{g_i + g_{iup}}{D^2} + \frac{2(f_i - f_{iup})}{D^3} , \quad (20)$$

$$b_i = \frac{3(f_{iup} - f_i)}{D^2} - \frac{2g_i + g_{iup}}{D} , \quad (21)$$

$$f_i^{n+1} = a_i S^3 + b_i S^2 + g_i^n S + f_i^n , \quad (22)$$

$$g_i^{n+1} = 3a_i S^2 + 2b_i S + g_i^n , \quad (23)$$

where $S = -c\Delta t$. Hence, $D = -\Delta s$, $iup = i - 1$ for $c \geq 0$ and $D = \Delta s$, $iup = i + 1$ for $c < 0$."

5 COMBINED METHOD OF FEM AND CIP

5.1 Numerical procedure in one dimensional problem

The boundary of FEM domain has to transmit various waves in order to analyze an infinite wave field. To realize this function, the CIP grid is overlapped to the FEM mesh efficiently around the boundary. We explain the basic procedure for the problem of one dimensional wave field by using an example of shear rod (Figure 1). The subscript *R* denotes the reflected wave from the free end which propagates in the direction of *x* axis, and the subscript *I* denotes the incident wave from the opposite direction. The superscripts *cip* and *fem* show the quantities on CIP grids and FEM nodes, respectively.

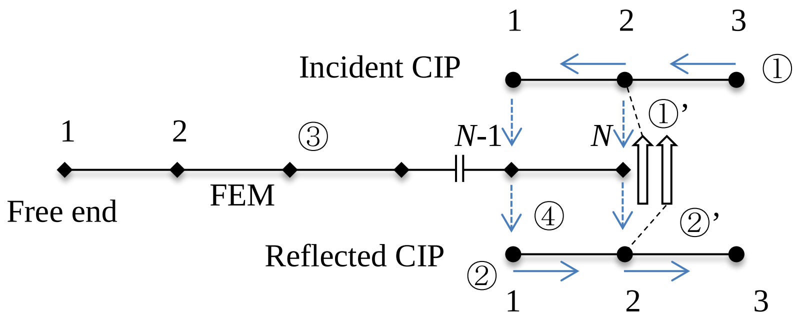

Figure 1: Analytical diagram

Two types of numerical procedures are summarized in the following.

(1) Tree Grids for CIP (High accuracy):

0-1. Make the time history of $f_{I3} = \frac{1}{2}\left(\frac{\dot{u}_{0I}}{c_s} + \frac{\tau_{0I}}{G}\right) = \frac{1}{2}\left(\frac{\dot{u}_{0I}}{c_s} + \frac{Gu'_{0I}}{G}\right) = \dot{u}_{0I}/c_s$

because $u'_{0I} = \dot{u}_{0I}/c_s$. ($\dot{u}_{0I}$: Incident velocity wave).

0-2. Initialize at all of the incident CIP grids: $f_{Ii}(0) = 0$ $(i = 1, 2, 3)$.

0-3. Initialize at all of the reflected CIP grids: $f_{Ri}(0)=0\ (i=1,2,3)$.

0-4. Set the initial condition at all of FEM nodes ($i=1,2,\cdots,N$)
: $u_i^{fem}(0)=\dot{u}_i^{fem}(0)=0$.

0-5. Set the time $t=0$.

1. Input $f_{I3}(t)$ at the incident CIP grid 3.

2. ①: Calculate $f_{Ii}(t+\Delta t)$ at the incident CIP grids: $i=1,2$ by $\dfrac{\partial f_I}{\partial t}-c_s\dfrac{\partial f_I}{\partial x}=0$.

3. ①': Evaluate the stress at the incident CIP grid 2 which is subjected to the FEM boundary node N as the external force
: $\tau_{I2}^{cip}(t+\Delta t)=Gf_{I2}(t+\Delta t)$

4. ②: Calculate $f_{Ri}(t+\Delta t)$ at the reflected CIP grids: $i=2,3$ by $\dfrac{\partial f_R}{\partial t}+c_s\dfrac{\partial f_R}{\partial x}=0$.

5. ②': Evaluate the stress at the reflected CIP grid 2 which is subjected to the FEM boundary node N as the external force
: $\tau_{R2}^{cip}(t+\Delta t)=Gf_{R2}(t+\Delta t)$

6. ③: FEM analysis by the linear acceleration method.
$[M]\{\ddot{u}^{fem}(t+\Delta t)\}+[C]\{\dot{u}^{fem}(t+\Delta t)\}+[K]\{u^{fem}(t+\Delta t)\}=\{\tau_{I2}^{cip}(t+\Delta t)\}+\{\tau_{R2}^{cip}(t+\Delta t)\}$

7. ④: Calculate $f_{Ri}(t+\Delta t)$ at the reflected CIP grids: $i=1,2$.
$$f_{Ri}(t+\Delta t)=\frac{1}{2}\left(-\dot{u}_{Ri}^{cip}(t+\Delta t)/c_s+\tau_{Ri}^{cip}(t+\Delta t)/G\right)=\frac{1}{2}\left(-\dot{u}_{Ri}^{fem}(t+\Delta t)/c_s+\tau_{Ri}^{fem}(t+\Delta t)/G\right)$$
because $\dot{u}_{Ri}^{cip}(t+\Delta t)=\dot{u}_{N-2+i}^{fem}(t+\Delta t)-\dot{u}_{Ii}^{cip}(t+\Delta t)=\dot{u}_{N-2+i}^{fem}(t+\Delta t)-c_s f_{Ii}(t+\Delta t)$.

8. Return to 1. after setting $t+\Delta t\rightarrow t$.

(2) One Grid for Incident CIP and Two Grids for Reflected CIP (High speed):

0-1. Make the time history of $f_{I2}=\dot{u}_{0I}/c_s$ ($\dot{u}_{0I}$: Incident velocity wave).

0-2. Initialize at the reflected CIP grids: $f_{Ri}(0)=0\ (i=1,2)$.

0-3. Set the initial condition at all of FEM nodes ($i=1,2,\cdots,N$)
: $u_i^{fem}(0)=\dot{u}_i^{fem}(0)=0$.

0-4. Set the time $t=0$.

1. ①': Evaluate the stress at the incident CIP grid 2 which is subjected to the FEM boundary node N as the external force
: $\tau_{I2}^{cip}(t+\Delta t)=Gf_{I2}(t+\Delta t)$

2. ②: Calculate $f_{R2}(t+\Delta t)$ at the reflected CIP grid 2 by $\dfrac{\partial f_R}{\partial t}+c_s\dfrac{\partial f_R}{\partial x}=0$.

3. ②': Evaluate the stress at the reflected CIP grid 2 which is subjected to the FEM boundary node N as the external force
   : $\tau_{R2}^{cip}(t+\Delta t) = Gf_{R2}(t+\Delta t)$
4. ③: FEM analysis by the linear acceleration method.
   $[M]\{\ddot{u}^{fem}(t+\Delta t)\}+[C]\{\dot{u}^{fem}(t+\Delta t)\}+[K]\{u^{fem}(t+\Delta t)\}=\{\tau_{I2}^{cip}(t+\Delta t)\}+\{\tau_{R2}^{cip}(t+\Delta t)\}$
5. ④: Calculate $f_{Ri}(t+\Delta t)$ at the reflected CIP grids: $i=1,2$.
   $$f_{Ri}(t+\Delta t) = \frac{1}{2}\left(-\dot{u}_{Ri}^{fem}(t+\Delta t)/c_s + \tau_{Ri}^{fem}(t+\Delta t)/G\right)$$
6. Return to 1. after setting $t+\Delta t \rightarrow t$.

Both of the procedures are also valid when the input motion is expressed as the incident acceleration wave. In this case, all of the above equations are differentiated.

5.2 Application to two and three dimensional problem

The procedure with one dimension is also used for the two and three dimensional problems by combining it with the flow of decomposition analysis explained in the section 3. Figure 2 shows how to generate the overlapping of FEM mesh and CIP grid in the two dimensional field.

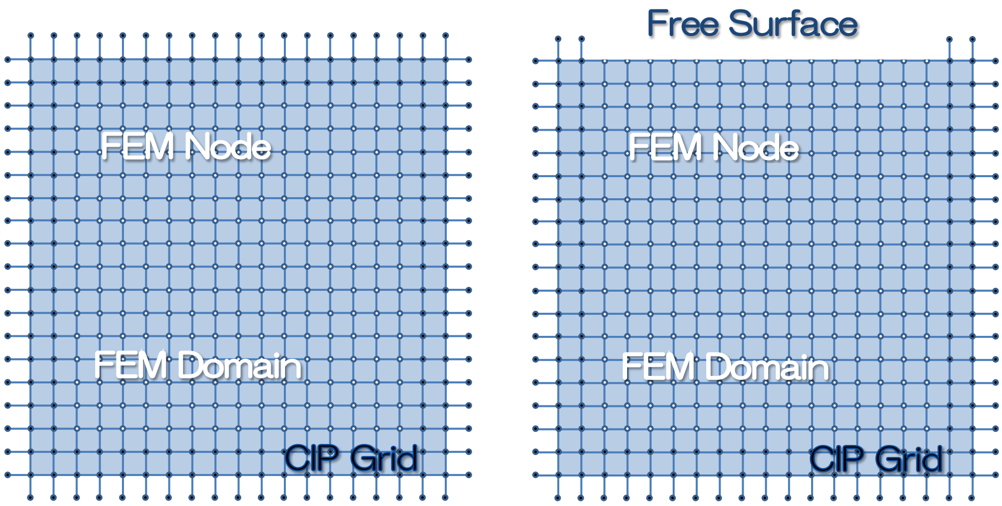

Figure 2: Overlapping of FEM mesh and CIP grid (Infinite space and half one)

6 NUMERICAL EXAMPLES

6.1 One dimensional field

The shear rod subjected to a half cycle velocity pulse at the right end, vibrates like Figure 3. The rod is divided into 40 elements with a linear interpolation on its displacement. In this paper, small Rayleigh dumping with 1.0% is introduced. Almost perfect transmission at the right end is realized after reflecting at the free end first.

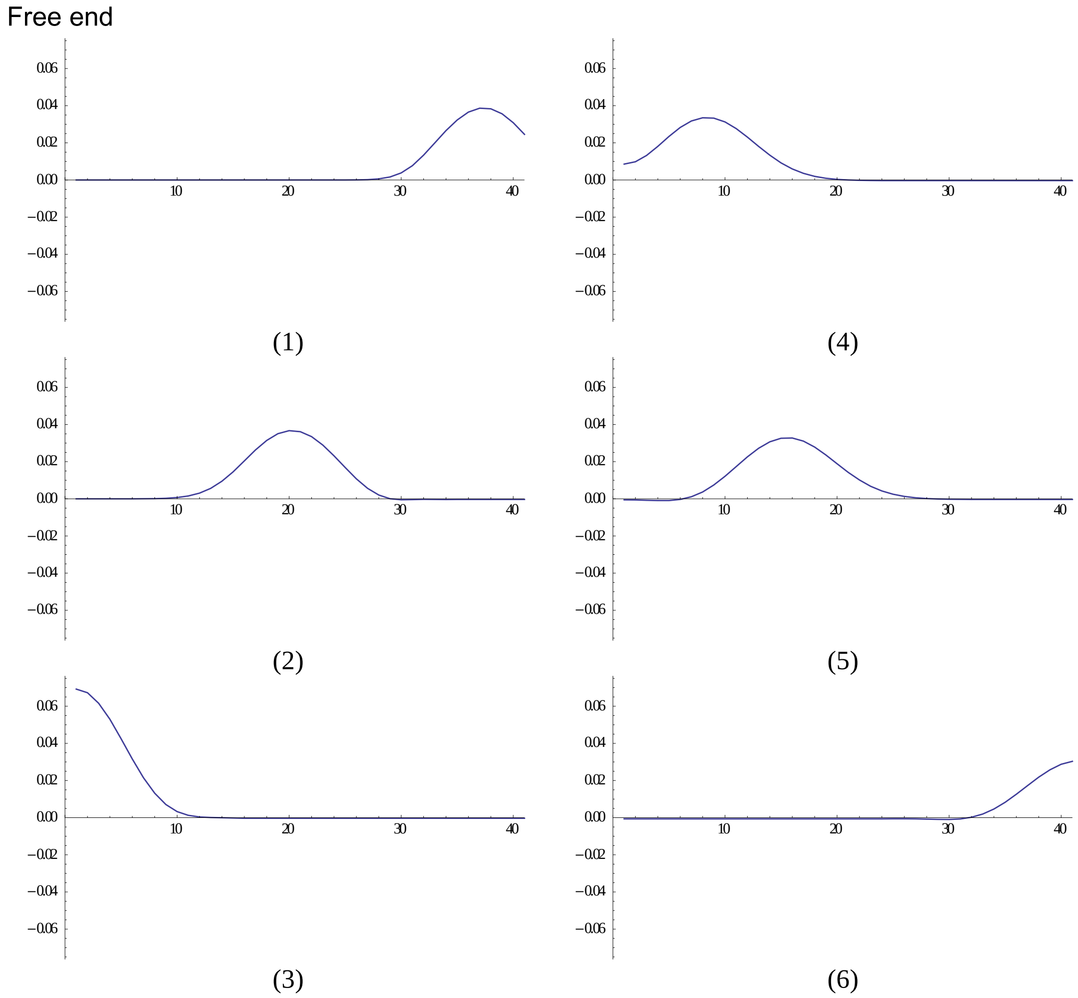

Figure 3: Shear rod subjected to a velocity pulse at the right end

6.2 Two dimensional field

The FEM mesh is 18×18 and the shape of its element is a rectangular with 4 nodes. Figure 4 shows the time history of the Kelvin problem that the cyclic point loading is applied in an infinite space. The boundary side of analytical fields is absorbing the outgoing wave perfectly.

Next, we show the wave field where SH wave incomes from the downward direction with the incident plus angle of 30-degree against vertical axis. In Figure 5, the incident wave of one cycle sine function is up-going toward the free surface and reflecting downward with a minus angle of the same.

Farther, in Figure 6 the embedded foundation is placed in soil. The incident wave collides with the edge of foundation. The high amplitude appears near the foundation at the free surface. Then the reflected wave diffracts around the foundation and dissipates download over the analytical boundary.

7 CONCLUSIONS

This paper proposed a new method for the transmitting boundary of the FEM domain based on CIP method. Its validity was shown by some numerical examples. In summary:

1. The transfer matrix $[T_{rs}]$ can be arranged to the same $[T]$, which is a powerful tool to convert the advection quantities of some direction to those of other directions.
2. Two kinds of CIP grid is used at the boundary of the FEM domain of which one is for the incident wave and another is for the reflected wave.
3. The number of nodes on CIP grid is at most two or three for every propagating direction.
4. The size of the FEM domain can be reduced as possible because the transmitting efficiency by CIP method is highly accurate.

REFERENCES

[1] Yabe, T. and Aoki, T. A universal solver for hyperbolic equations by cubic-polynomial interpolation. *Computational Physics Commun*. (1991) **66**:219–242.

[2] Teramoto, K. 3-dimensional elastic wave field simulation by CIP method, *Techniacl Report of IEICE* (2005) EA**2004-131**:39-44 (in Japanese).

[3] Yabe, T. and et al. Higher-order schemes with CIP method and adaptive Soroban grid towards mesh-free scheme. *Journal of Computational Physics Computational Physics* (2004) **194**:57–77.

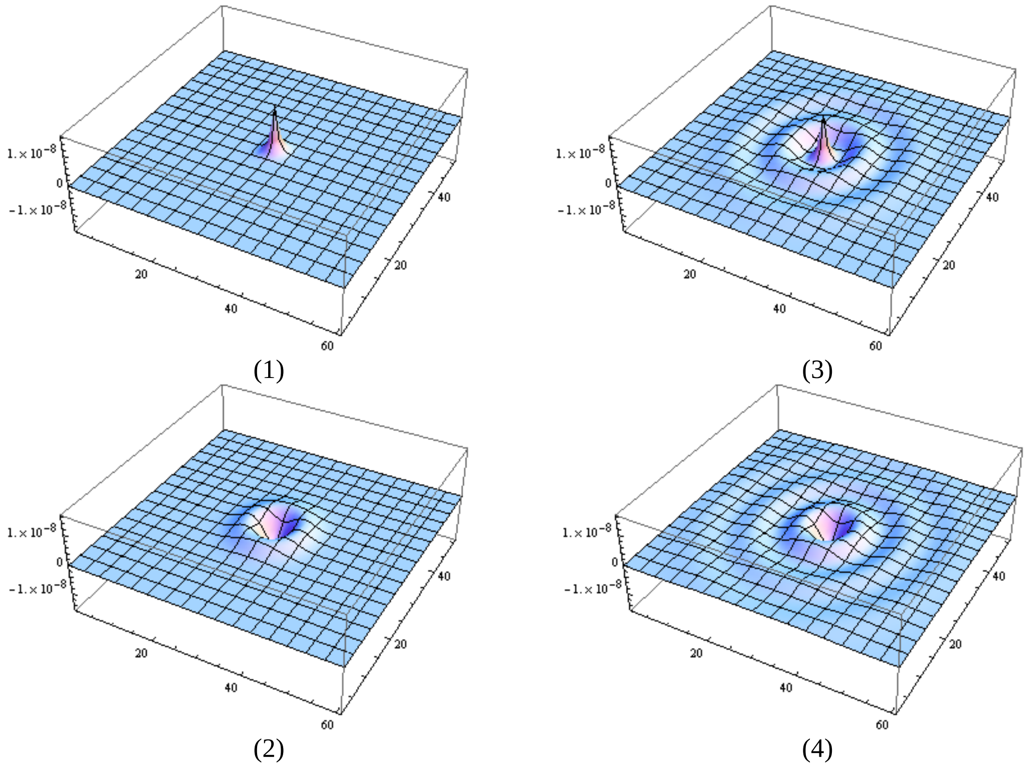

Figure 4: Kelvin problem in in-plane field of two dimensional space

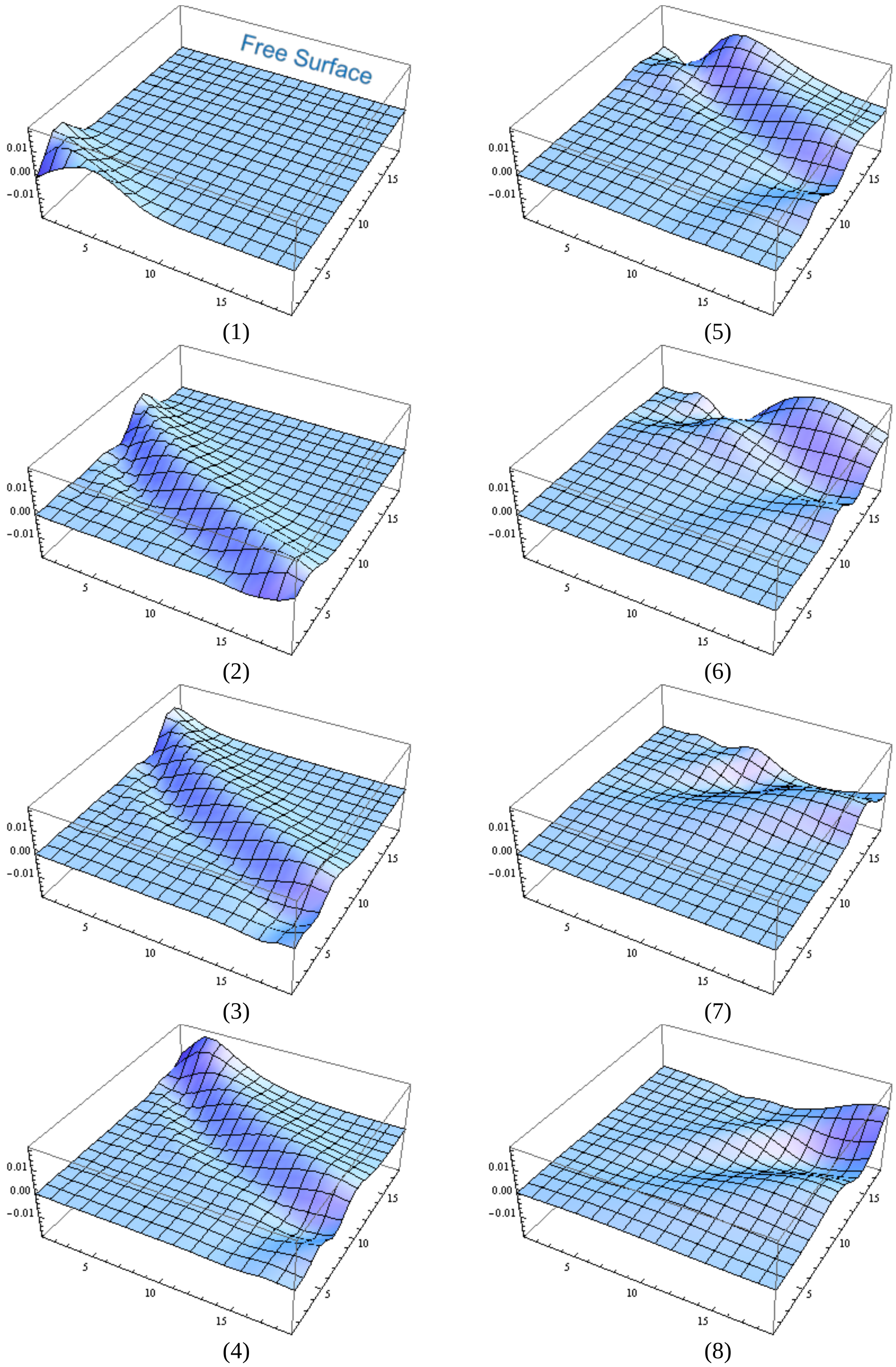

Figure 5: Two dimensional free field of half space subjected to SH wave with incident angle of 30-degree

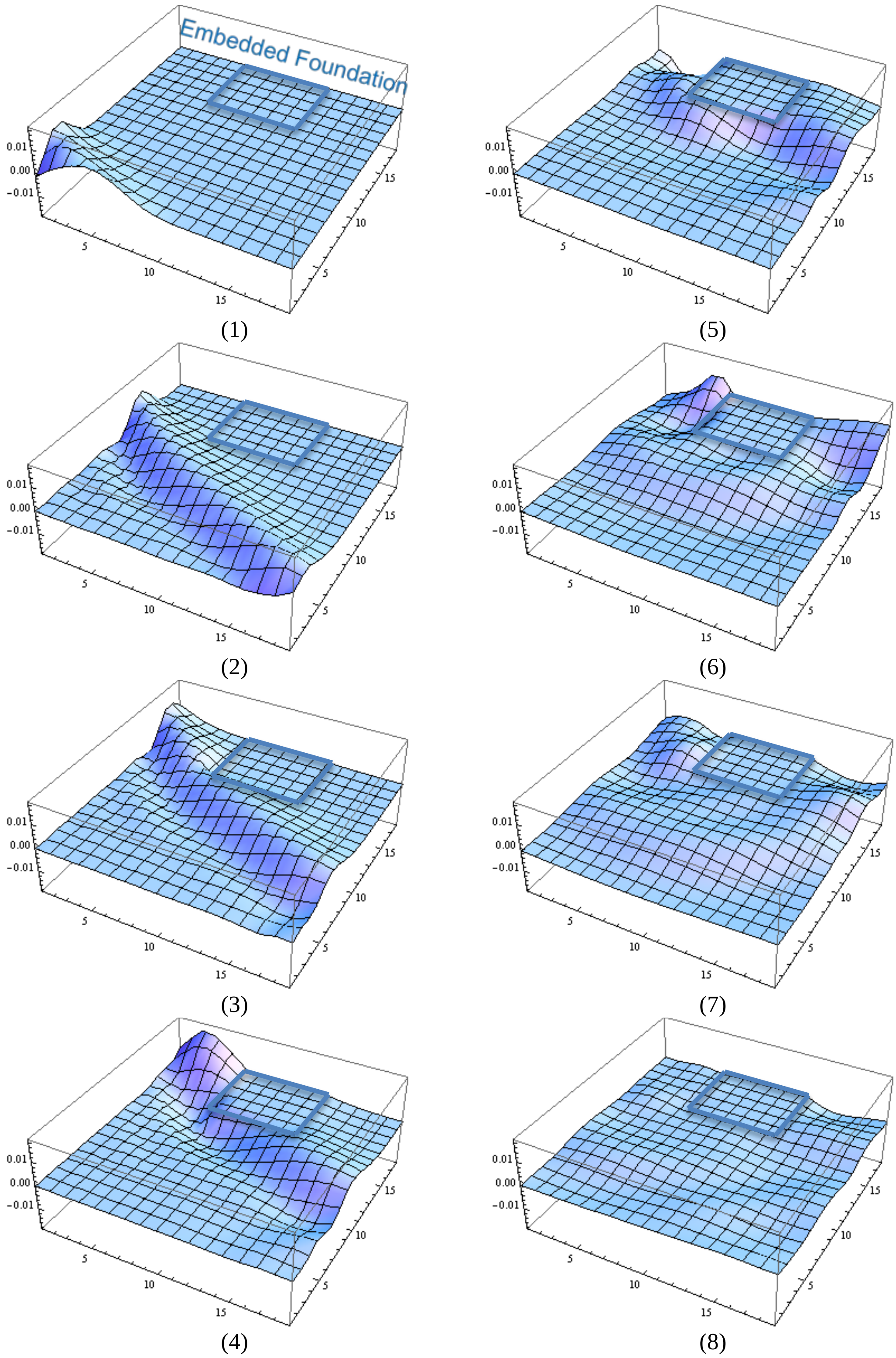

Figure 6: Embedded foundation subjected to SH wave with 30-degree of incident angle